Elucidating the impacts of aerosol radiative effects on surface O_3 and $PM_{2.5}$ for air pollution mitigation strategy in Delhi, India

Lakhima Chutia[1, 2]*, Jun Wang[1, 2]*, Huanxin Zhang[1, 2], Lorena Castro Garcia[1, 2], Nathan Janechek[2]

[1]Department of Chemical and Biochemical Engineering, College of Engineering, University of Iowa, IA, USA

[2]Iowa Technology Institute and Global and Regional Environmental Research, College of Engineering, University of Iowa, IA, USA

*Corresponding author: Jun Wang, jun-wang-1@uiowa.edu;
Lakhima Chutia, lakhima-chutia@uiowa.edu

Key points:

- The aerosol–photolysis effect contributes to a reduction in surface O_3 and $PM_{2.5}$ concentration in Delhi during post-monsoon.
- The aerosol–radiation feedback decreases the boundary layer mixing, increases relative humidity, and aggravates surface $PM_{2.5}$ and O_3.
- Effective control of VOC helps in achieving both O_3 and $PM_{2.5}$ reductions in Delhi.

Abstract

Atmospheric aerosol radiative effects regulate surface air pollution (O_3 and $PM_{2.5}$) via both the aerosol–photolysis effect (APE) and the aerosol–radiation feedback (ARF) on meteorology. Here, we elucidate the roles of APE and ARF on surface O_3 and $PM_{2.5}$ in the heavily polluted megacity, Delhi, India by using a regional model (WRF-Chem) with constraints from available and limited observation. While APE reduces surface O_3 (by 6%) and $PM_{2.5}$ concentrations (by 2.4% via impeding the secondary aerosol formations), ARF contributes to a 17.5% and 2.5% increase in surface $PM_{2.5}$ and O_3, respectively. The synergistic APE and ARF impact contributed to ~1 % of the total concentrations of O_3 and $PM_{2.5}$. Hence, the reduction of $PM_{2.5}$ may lead to O_3 escalation due to weakened APE. Sensitivity experiments indicate the need and effectiveness of reducing VOC emission for the co-benefits of mitigating both O_3 and $PM_{2.5}$ concentrations in Delhi.

Plain Language Summary

Surface ozone (O_3) and fine particulate matter ($PM_{2.5}$) are dominant air pollutants in the megacity Delhi, India. However, controlling $PM_{2.5}$ concentration by reducing emissions may have unexpected consequences on O_3 because aerosols may lead to O_3 escalation by increasing photolysis and at the same time reduce O_3 by increasing the solar input at the surface and hence, the turbulent mixing. Here we used a regional model to quantify the separate contribution of aerosol–photolysis effect (APE) and aerosol–radiation feedback (ARF) on surface $PM_{2.5}$ and O_3 in Delhi and further discuss the measures for reducing both $PM_{2.5}$ and O_3 levels. This study elucidates the importance of APE and ARF effects in designing effective mitigation strategies for both $PM_{2.5}$ and O_3 pollution. The effective control of VOC emissions is highly recommended for co-controlling both O_3 and $PM_{2.5}$ levels in the megacity Delhi.

1 Introduction

Ground-level ozone (O_3) and fine particulate matter with aerodynamic diameter ≤2.5 μm or $PM_{2.5}$ are dominant air pollutants in megacities such as Delhi, India. Delhi has been experiencing severe air pollution episodes in recent years, especially during the post-monsoon (Oct. and Nov.) and winter times (Dec., Jan., and Feb.) (Bharali et al., 2019; Kulkarni et al., 2020; Kumar et al., 2020). $PM_{2.5}$ and O_3 in this region often exceed the Indian National Ambient Air Quality Standards (INAAQS) and pose a serious threat to public health (Ghude et al., 2016; Krishna et al., 2019; Sahu & Kota, 2017). $PM_{2.5}$ can lead to ~ 1 million premature deaths per year in India (Conibear et al., 2018; Ghude et al., 2016). O_3, the second major pollutant adversely impacting human health after $PM_{2.5}$ also leads to 31,000 premature mortalities per year (Ghude et al., 2016). Besides, O_3 and $PM_{2.5}$ exposure damages crops and significantly reduces wheat and rice (22–42%) yields in India (Sinha et al., 2015). Therefore, the prediction and process understanding of both $PM_{2.5}$ and O_3 are highly essential to improve the air quality and mitigate their impacts on public health and agriculture in this region.

Past studies have focused on several factors including emission, meteorology, and atmospheric chemistry governing the high concentrations of $PM_{2.5}$ and O_3 in the Indian region (Bran & Srivastava, 2017; Kulkarni et al., 2020; Ojha et al., 2020). One factor often overlooked in the literature is the impact of aerosol–radiation interaction (ARI) on both $PM_{2.5}$ and O_3 and the non-linear synergistic processes therein. The ARI influences O_3 chemistry and atmospheric oxidation capacity by modulating photolysis rates in the troposphere known as the aerosol–photolysis effect (APE) which further influences the particle formation process and air quality (Benas et al., 2013; Dickerson et al., 1997; Li et al., 2011; Liao et al., 1999; Xing et al., 2017). Modeling studies have highlighted the reduction (enhancement) in photolysis rate due to strong absorption (scattering) of aerosols (Li et al., 2005; Li et al., 2017; Liao et al., 1999, Tie et al., 2003), with subsequent effects on the O_3 formation. Several studies have analyzed the impact of APE in different parts of the world such as the urban environment in China (Xing et al., 2017; Yang et al., 2022), Mexico (Li et al., 2011), Europe (Real & Sartelet, 2011), and Texas (Flynn et al., 2010). However, such studies are still limited over the Indian region.

ARI not only entails APE but also includes aerosol–radiation feedback or ARF on meteorology that in turn affects surface O_3 and aerosol distribution. ARI can lead to a substantial decrease of solar inputs at the ground, thereby reducing surface temperature and the planetary

boundary layer (PBL) height. Via absorption of radiation, aerosols can heat the atmosphere, increase atmospheric stability, and further enhance aerosol concentration in the PBL (Li et al., 2017; Yang et al., 2020); this positive feedback via ARF is particularly significant during severe pollution episodes (Bharali et al., 2019; Liu et al., 2018; Wang et al., 2020; Zhao et al., 2019).

To study the air pollution mitigation strategy in Delhi, India, here we employ a regional chemistry transport model (WRF-Chem) to elucidate the relative role of APE and ARF on surface $PM_{2.5}$ and O_3 in the National Capital Region (NCR) of India. WRF-Chem has been widely used for the simulation of $PM_{2.5}$ and O_3 across the Indian region (Bran & Srivastava, 2017; Jat et al., 2021; Mogno et al., 2021; Ojha et al., 2020; Sharma et al., 2017; Upadhyay et al., 2018). But only a few studies have focused on the impacts of ARF (Kumar et al., 2020; Bharali et al., 2019) with no study analyzing the pure and synergistic effect of APE and ARF. Kumar et al. (2020) showed that the inclusion of ARF in WRF-Chem can lead to a significant improvement in the $PM_{2.5}$ forecast by reducing the mean bias up to 25% in NCR Delhi. Mukherjee et al. (2020) found a 30% reduction in surface O_3 concentration due to the APE associated with black carbon over South Asia. Hence, while reducing black carbon may lead to a decrease in $PM_{2.5}$, it may lead to an increase in surface O_3 concentration. The overall net effects of APE and ARF on both O_3 and $PM_{2.5}$ over the Indian region remain elusive, although the air pollution mitigation strategy requires scientific consideration of the role of both APE and ARF as well as their synergistic effects.

Here, the pure and synergistic contributions of APE and ARF are quantitatively analyzed through model sensitivity simulations with the constraint of surface observations (described in section 2.2), focusing on the post-monsoon period in November 2018 over NCR Delhi. Results are presented in Section 3, starting from the comparison of the model results with observations (Section 3.1) to the analysis of the impact of pure and synergistic APE and ARF (Section 3.2–3.3). The summary and conclusions are provided in Section 4.

2 Methodology

2.1 Model Description

A regional model with Unified Inputs (of initial and boundary conditions) for the Weather Research and Forecasting model coupled with chemistry (UI-WRF-Chem) is used to simulate O_3 and $PM_{2.5}$ in Delhi in two nested domains at 12 and 4 km horizontal resolutions,

respectively. The outer and inner domains cover the entire northern part of the Indian subcontinent and NCR Delhi, respectively (Figure S1). There are 47 vertical layers from the ground to 50 hPa. The UI-WRF-Chem model utilizes MERRA-2 data to provide both meteorological and chemical initial and boundary conditions. Initial conditions for soil properties (soil moisture, soil temperature) are taken from the Global Land Data Assimilation System (GLDAS) at a horizontal resolution of 0.25° × 0. 25°.

The WRF-Chem emission preprocessing system (WEPS) designed in-house is used to prepare the anthropogenic and biogenic emissions needed for UI-WRF-Chem (Sha et al., 2021; Zhang et al., 2022). Anthropogenic emissions are based on Emissions Database for Global Atmospheric Research - Hemispheric Transport of Air Pollution (EDGAR-HTAP) (Janssens-Maenhout et al., 2015), which includes PM_{10}, $PM_{2.5}$, BC, OC, NH_3, NMVOCs, CO, NOx and SO_2 at a horizontal resolution of 0.1º x 0.1º. Biomass burning emissions from the Fire Locating and Modeling of Burning Emissions Inventory (FLAMBE) (Reid et al., 2009) is used to specify the sources of BC, OC, and gaseous species (CO, NO_2) as a function of time (at injection height of 800 m above the surface). Further details of FLAMBE and WEPS can be found elsewhere (Ge, Wang, & Reid, 2013; Ge et al., 2017; Wang et al., 2013). Regional Acid Deposition Model version 2 (RADM2) (Stockwell et al., 1990) coupled with the Modal Aerosol Dynamics for Europe (MADE) and the Secondary Organic Aerosol Model (SORGAM) (Schell et al., 2001) are used to simulate the gas-phase chemistry and aerosols. Currently, the inorganic chemistry system considered in MADE is limited to sulfate, nitrate, ammonium, and water components in the aerosol phase. The Fast Tropospheric UV and Visible Radiation Model (FTUV) (Li et al., 2005; Tie et al., 2003) is used to evaluate aerosol effects on photolysis rates and the Goddard shortwave radiative transfer module (Chou & Suarez, 1994) is employed for estimating shortwave radiation. Other physics parameterization schemes (Table S1) used here are based on the earlier studies using the WRF-Chem model over the Indian region (Chutia et al., 2019; Ojha et al., 2020).

2.2 Simulation scenarios and analysis method

We utilized the factor separation approach (FSA) method (Stein & Alpert, 1993) to obtain the pure contribution of APE and ARF and their synergistic contributions due to the mutual interactions among APE and ARF. This method has been extensively applied in the analysis of

numerical simulations (Li et al., 2018; Qu et al., 2013). Based on the FSA, four simulations such as BASE, NOALL, APE only, and ARF only, have been performed to quantify the pure and synergistic impacts of APE and ARF on O_3 and $PM_{2.5}$ (See Table S2). In the BASE simulation, the impacts of both ARF and APE are considered. In NOALL, ARF and APE are both turned off. Considering that $f_{ARF+APE}$, f_{ARF}, f_{APE}, and f_0 are the simulation results including both APE and ARF (i.e., BASE), ARF only, APE only, and neither APE nor ARF (i.e., NOALL), respectively, one can show that the synergistic contributions between APE and ARF are as follows:

$$f'_{ARF+APE} = f_{ARF+APE} - f_{APE} - f_{ARF} + f_0 \quad \text{(i)}$$

Each simulation is performed from 22 October to 30 November 2018 with the first 10 days as the model spin up.

2.3 Observational Data

Ground-based measurements of $PM_{2.5}$, O_3, and meteorological parameters (temperature and relative humidity) at different stations over NCR Delhi (Figure S1b) are obtained from the Central Pollution Control Board (CPCB), India. The instruments are periodically calibrated, and measurements are regularly checked and controlled with quality assurance by the CPCB (cpcb.nic.in/quality-assurance-quality-control/). Additional data assurance is considered by removing very high (> 1500 mg m^{-3}) and low (< 10 mg m^{-3}) $PM_{2.5}$ values following Kumar et al (2020).

3 Results

3.1 Model evaluation

The BASE and NOALL simulations are first used for the evaluation of overall impact of ARI on the model results. The diurnal pattern and magnitude of 2 m air temperature (T2) and relative humidity (RH) are captured well by the UI-WRF-Chem in both simulations, with a relatively smaller bias in the BASE case (Figure 1a–b and Table S3). The normalized mean bias (NMB) between the observation and model is reduced from –11% in NOALL to –5% in the BASE for RH and 5% to 2% for T2.

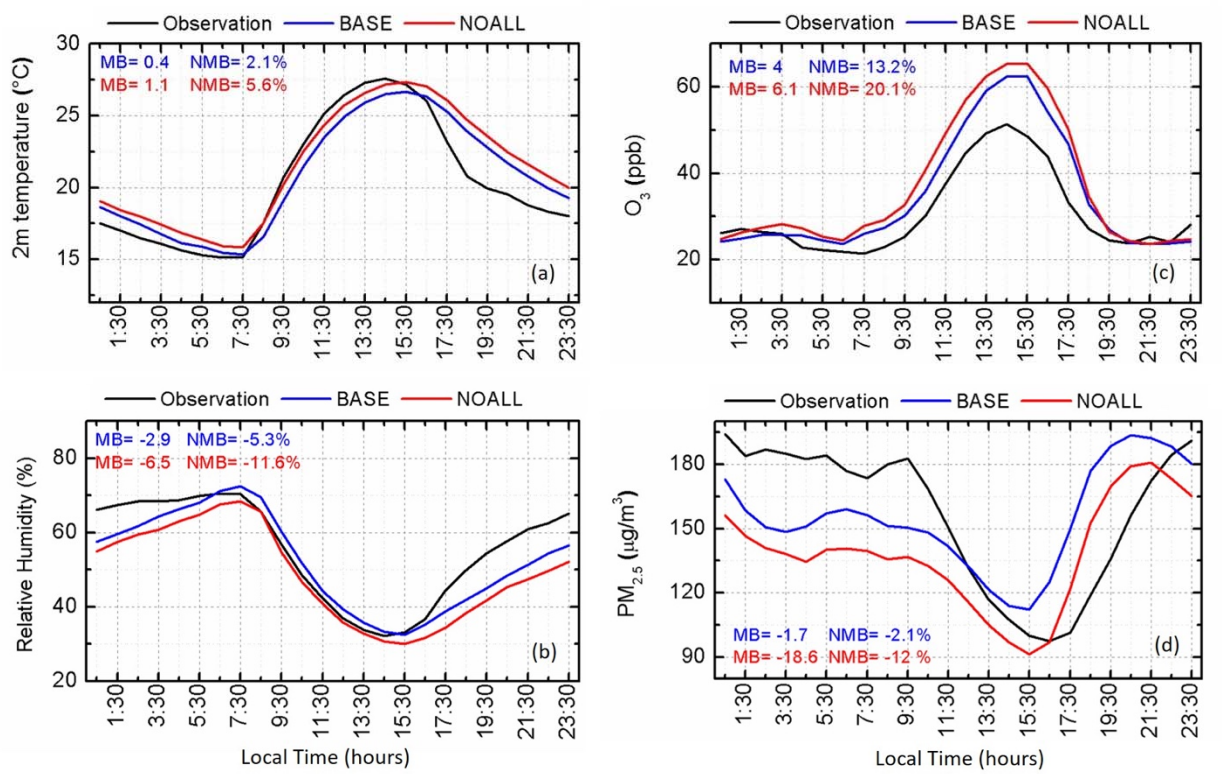

Figure 1. Diurnal variation of observed (black) and simulated variables (blue for BASE and red for NOALL experiments). **(a)** 2m temperature (° C), **(b)** relative humidity (%), **(c)** O_3 (ppb), and **(d)** $PM_{2.5}$ (µg m^{-3}) in megacity Delhi during November 2018.

Figures 1(c–d) illustrate the monthly averaged diurnal variation of observed and simulated surface $PM_{2.5}$ and O_3 concentrations in megacity Delhi during November 2018. The UI-WRF-Chem captured the observed diurnal variations of surface O_3 and $PM_{2.5}$ with a good correlation (of 0.96 – 0.97 and 0.52 – 0.62, respectively) in both BASE and NOALL simulations (Figure 1c–d and Table S3). However, the model overestimates the daytime O_3 peak in both simulations (MB of 16 ppb in the NOALL case), with relatively less bias in the BASE case (MB of 11 ppb). Additionally, the peak of the observed $PM_{2.5}$ mass related to the morning rush hour traffic emissions is not captured well by the UI-WRF-Chem. Nevertheless, the modeled correlation of diurnal variation with observation has coefficients of 0.52 – 0.62. The differences between the model and observation could be associated with uncertainties in the input emissions, boundary layer processes, meteorology, and chemical processes. Furthermore, the absolute levels of O_3 and $PM_{2.5}$ simulated here are also consistent with the earlier model-based studies in this region (Hakim et al., 2019; Ojha et al., 2020). However, the model performed better in the BASE

experiment i.e., when both the APE and ARF are considered. The overall NMB between the model and observed O_3 is reduced from 20% in NOALL to 13% in the BASE experiment. Similarly, the NMB decreased from 12% in NOALL to 2% in the BASE simulation for $PM_{2.5}$. This supports previous findings by Kumar et al. (2020) where they have reported that ARF can lead to ~21–25% reduction in the mean bias of the $PM_{2.5}$ forecast in Delhi; however, the APE effects on O_3 and the synergistic APE and ARF effects were not quantified in their study. The contrast between BASE and NOALL suggests that UI-WRF-Chem has the fidelity needed to study the role of APE and ARF toward the improvement of UI-WRF-Chem simulation of surface O_3 and $PM_{2.5}$.

3.2 Pure contribution of APE and ARF

Figures 2(b, c, f, g, j, k) and Table 1 illustrate the pure contribution of APE and ARF on surface O_3, NO_2, and $PM_{2.5}$ concentrations over NCR Delhi. The pure APE contributed to a reduction in the O_3 concentration by 3.29 ppb (6.1%) via weakening the efficiency of the photolytic reaction. In the pure APE scenario, the surface photolysis rates $J[NO_2]$ and $J[O^1D]$ are decreased by ~23% over NCR Delhi (Figure S2a, d, Table1) which in turn reduces the surface O_3 and OH radical concentration (Figure S2g). The reduction in $J[NO_2]$ and $J[O^1D]$ is particularly significant (Figure S3) during the early morning (07:30 – 08:30 LT) and late afternoon hours (15:30 –16:30 LT, i.e., when the solar zenith angle is at around 60°), signifying the influence of long path length of aerosol optical extinction for incoming UV radiation (Li et al., 2011). In contrast, the pure impact of ARF increases surface O_3 over most areas of the simulated domain by up to 3 ppb but slightly decreases in the megacity Delhi by up to 0.5 ppb. Overall ARF increases the surface O_3 by 2.5% over the entire simulated domain (Figure 2c). This results primarily from the reduction of the boundary layer height and surface energy budget by ARF (Figure S4). The aerosol-induced solar dimming (–47 Wm^{-2}) leads to a cooling of –1°K at the surface and decreases the surface wind speed (–0.11 ms^{-1}) and the noontime boundary layer by ~143 m over the simulated domain (Figure S4). The reduced ventilation due to the shallower atmospheric boundary layer and weaker winds caused by the ARF enhances the precursor levels resulting in greater O_3 chemical formation. Contrarily, in megacity Delhi, which is a VOC-limited regime (Nelson et al., 2021), increased NOx (see Figure 2g) concentrations at the surface associated with the ARF inhibit O_3 formation due to the enhanced titration by NO. However, the

209 O_3 reduction due to ARF in megacity Delhi is far less significant than the changes caused by
210 APE.

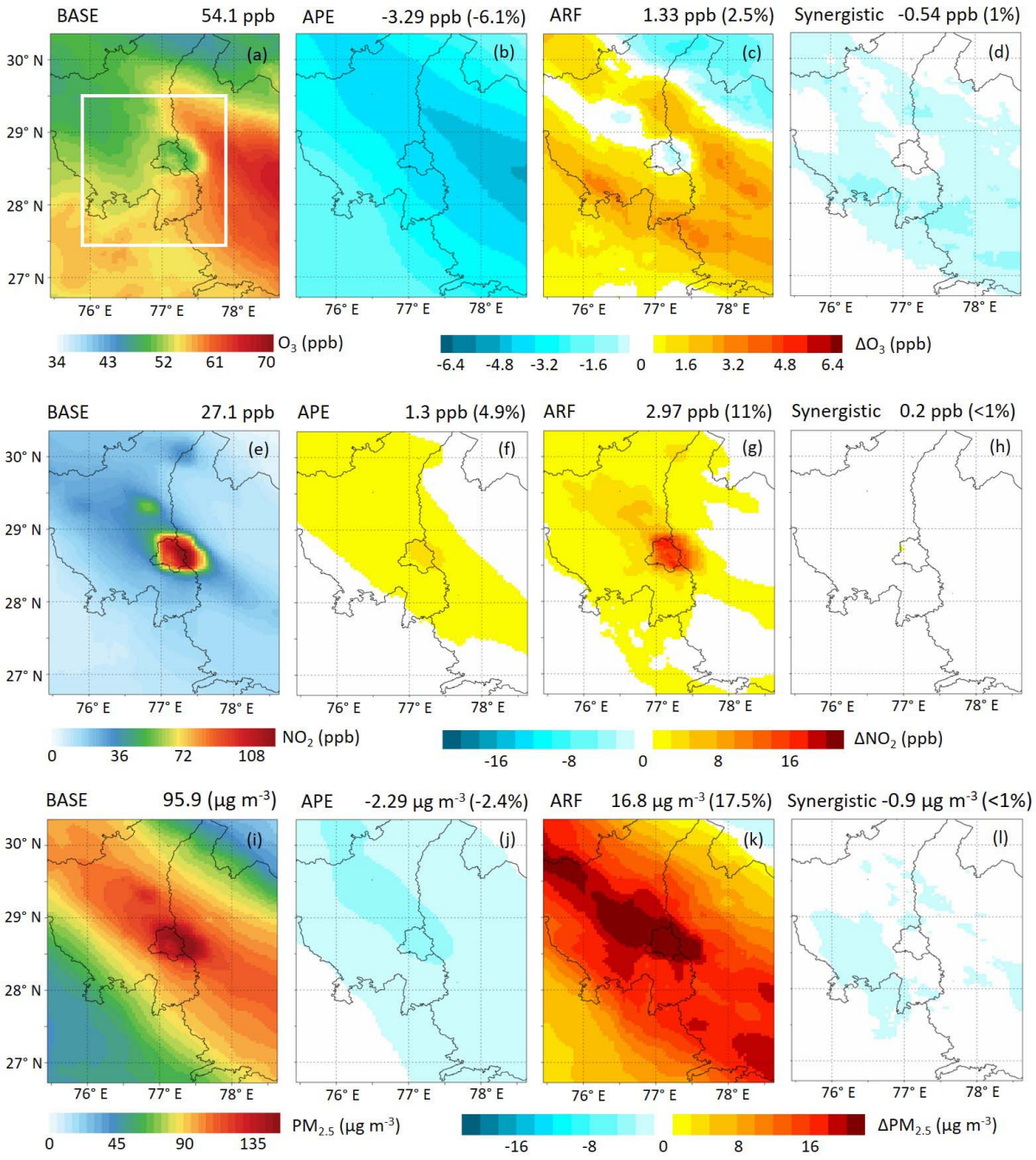

211

212 **Figure 2.** Spatial distribution of the monthly mean concentrations of O_3 (upper panel), NO_2
213 (middle panel), and $PM_{2.5}$ (lower panel) averaged during the daytime (07:30–17:30 LT) in
214 November 2018. (**a, e, i)** are from BASE simulation; **(b, f, j)** are the change of concentrations
215 due to the pure APE, **(c, g, k)** are similar to (b, f, j) but due to the pure ARF, and (**d, h, l)** are the

changes due to the synergistic APE and ARF. The calculated values averaged over NCR Delhi (denoted as white box panel (a)) are shown at the top of each panel.

Contribution	O_3 (ppb)	$PM_{2.5}$ ($\mu g\ m^{-3}$)	NO_2 (ppb)	Sulfate ($\mu g\ m^{-3}$)	Nitrate ($\mu g\ m^{-3}$)	Ammonium ($\mu g\ m^{-3}$)	$J[NO_2]$ ($10^{-3}\ s^{-1}$)	$J[O^1D]$ ($10^{-6}\ s^{-1}$)	OH (ppt)
BASE	54.11	95.9	27.14	4.258	40.175	13.29	3.898	9.519	0.075
Pure ARF	1.33	16.77	2.97	0.26	10.397	3.118	0.003	–0.084	–0.0068
Pure APE	–3.29	-2.29	1.3	-0.25	–1.60	–0.558	–0.872	–2.26	–0.024
Synergistic APE & ARF	–0.54	–0.89	0.2	-0.029	–0.64	–0.197	–0.024	–0.044	–0.0007

Table 1. Pure and synergistic contributions of APE and ARF on O_3, $PM_{2.5}$, NO_2, SNA, photolysis rates, and OH radical concentration

In the case of $PM_{2.5}$, pure ARF contributed substantially to the $PM_{2.5}$ accumulation near the surface with an average contribution of 17.5 % (16.8 $\mu g\ m^{-3}$) over the simulated domain (Figure 2k). The pure impact of ARF on $PM_{2.5}$ is prominent in the megacity Delhi contributing more than 20%. The increased atmospheric stability due to the pure ARF hinders the $PM_{2.5}$ dispersion and subsequently aggravates $PM_{2.5}$ pollution near the surface. On the other hand, pure APE inhibits the $PM_{2.5}$ concentrations and leads to a decrease of 2.4% (2.29 $\mu g\ m^{-3}$). To corroborate this finding, changes in the secondary inorganic aerosols such as sulfate, nitrate, and ammonium (SNA) in the pure ARF and APE scenarios are analyzed (Figure S5). Bawase et al. (2021) reported that SNA ions ($31.44 \pm 20.69\ \mu g\ m^{-3}$) are one of the largest contributors to $PM_{2.5}$ along with organic matter in Delhi. SNA are mostly produced in the atmosphere through oxidation (including OH, and NO_3 emitted from the photolysis reactions) and neutralization of precursor gases (such as SO_2, NO_2, and NH_3). As seen in Figure S5 and Table 1, pure ARF substantially enhances the surface SNA concentration while pure APE leads to a slight reduction. On average, sulfate, nitrate, and ammonium concentrations are increased by 0.26 $\mu g\ m^{-3}$ (6.1%), 10.4 $\mu g\ m^{-3}$ (25.9%), and 3.1 $\mu g\ m^{-3}$ (23%), respectively due to pure ARF. The extent of SNA changes due to APE is relatively smaller than the changes caused by the pure ARF effect. Pure APE decreases sulfate, nitrate, and ammonium concentration by 0.25 $\mu g\ m^{-3}$ (5.9%), 1.6 $\mu g\ m^{-3}$

(4%) and 0.56 μg m^{-3} (4.2%), respectively. The lower abundances of atmospheric oxidants due to the modification of photolysis by pure APE decreases the rate of SNA formation and subsequently alleviates the $PM_{2.5}$ concentrations near the surface.

3.3 Synergistic contribution of APE and ARF

The synergistic impact includes the mutual interactions between the APE and ARF. Figures 2(d, h, l) illustrate the synergistic contribution of APE and ARF on surface O_3, NO_2, and $PM_{2.5}$ concentrations. The synergistic APE and ARF result in an overall decrease of –0.54 ppb (1%) in the monthly mean surface O_3 concentration averaged during the daytime (07:30–17:30 LT). In the case of daily peak (13:30–16:30 LT) O_3, the synergistic APE and ARF contributed –0.8 ppb of total concentration (Figure S6d). However, in VOC-limited regimes such as in megacity Delhi, the synergistic impact is nearly insignificant (<0.5%) (Figures 2d and S6d). Similarly, the synergistic APE and ARF have negligible effect on modifying the photolysis rates (<0.5%) (Figure S2c, f) and consequently little impact on the OH radical (1%) (Figure S2i) and secondary particulate concentration (< 2%) (Figures S5 d, h, l). In the case of NO_2 and $PM_{2.5}$, the synergistic impact contributed less than ±1 % of the total concentrations. Overall, the calculated synergistic impact of APE and ARF contributed very little to the O_3 and $PM_{2.5}$ concentrations and the impact is far less significant than pure APE and ARF impact.

3.4 Discussions

Figure S7 summarizes the different pathways of APE and ARF affecting O_3 and $PM_{2.5}$. The ARF cools the surface, reduces turbulent mixing, and is conducive to the increase of relative humidity (see Figure S4g), all of which are contributory to the enhancement in surface $PM_{2.5}$ and precursor gas concentration. The enhanced chemical loss via strong NO titration effect ($NO + O_3 \rightarrow NO_2 + O_2$) associated with the high NOx emissions plays a critical role in weakening O_3 production in the megacity Delhi.

In the case of pure APE, the weakening O_3 and OH concentration further impedes the secondary aerosol formations and subsequently alleviates the near-surface $PM_{2.5}$ concentrations. A substantial reduction (~23%) in surface $J[NO_2]$ due to APE has been observed in Beijing, China during haze events further hindering the secondary aerosols (3.5–9.4%) and $PM_{2.5}$ (4.2%) concentrations (Wu et al., 2020), which is consistent with our results. The pure contributions of

APE and ARF on surface O_3 as a function of $PM_{2.5}$ in megacity Delhi (See Figure S8) further show that the extent of O_3 changes due to APE is larger than ARF. The APE-induced O_3 reduction is higher when surface $PM_{2.5}$ can reach high levels larger than 180 μg m^{-3} (Figure S8). Relatively strong APE effects on the surface O_3 formation compared to ARF have also been reported in North China (Yang et al., 2022); however, the synergistic effects were not quantified in their study.

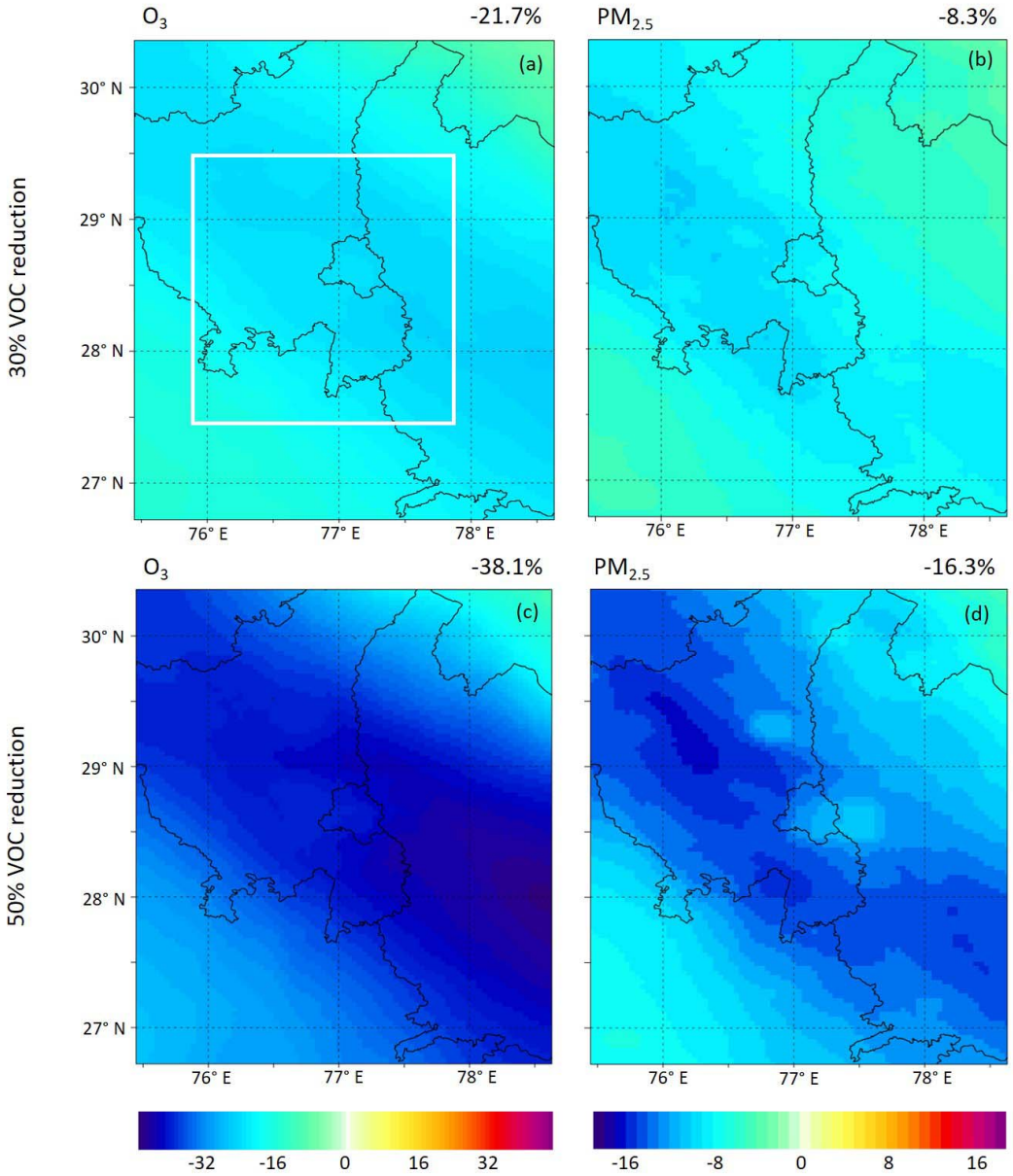

Figure 3. (a, c) O_3 and **(b, d)** $PM_{2.5}$ responses to the 30% and 50% reduction of VOC emissions over NCR Delhi in November 2018.

Overall, the elucidation of the role of APE and ARF shows the importance of a simultaneous mitigation strategy to co-control both O_3 and $PM_{2.5}$ concentrations in the megacity Delhi. The results suggest that $PM_{2.5}$ reduction may lead to O_3 escalations due to the weakened ARI. Since surface O_3 formation in Delhi is VOC limited and VOCs are common precursors for both O_3 and $PM_{2.5}$, effective control of VOC emissions is required to counterbalance future O_3 escalations. To examine the O_3 and $PM_{2.5}$ responses to VOC emission reduction, we have performed two more sensitivity experiments by reducing VOC anthropogenic emissions by 30% and 50% (Figure 3 and Figure S9). The 30% VOC reduction scenario showed a decrease in surface O_3 concentration by 21% over NCR Delhi. The O_3 decrease became 38% in the 50% VOC emission reduction scenario and leads to a large decrease (48%) in the OH radical concentration (Figure S10). As OH is the key reactive species in the formation of secondary inorganic aerosols, the reduction in VOC emissions by 30–50% reduces the sulfate, nitrate, and ammonium concentration by 12–26% (See Figure S11). As a result, the 30% and 50% reduction of VOC leads to a decrease in $PM_{2.5}$ concentration by 8% and 16%, respectively over NCR Delhi (Figure 3b, d). A recent analysis over Delhi (Chen et al., 2020) showed that a reduction in local traffic emission by 50% alone reduces $PM_{2.5}$ concentration by 15–30% in Delhi but increases O_3 by 20–25%. However, the reduction in emissions of regional transport of pollution from the NCR surrounding Delhi by 25–30% at the same time while reducing traffic emissions in Delhi would further reduce $PM_{2.5}$ by 5–10% and avoid the O_3 increase (Chen et al., 2020) in line with our result. Our study suggests that effective control of VOC emission helps in achieving O_3 reduction directly and also indirectly via weakening ARF effects from the reduced $PM_{2.5}$, emphasizing the need and efficacy of VOC control for simultaneous mitigation of O_3 and $PM_{2.5}$ in Delhi.

4 Summary and conclusions

The pure and synergistic impacts of APE and ARF on surface O_3 and $PM_{2.5}$ are quantified using a regional model UI-WRF-Chem employing the FSA method over NCR Delhi in November 2018. The model performance in simulating surface O_3 and $PM_{2.5}$ is improved after the inclusion of ARI (both APE and ARF) with a significant reduction in mean bias in the megacity Delhi. The results reveal that APE reduces the surface O_3 and $PM_{2.5}$ concentrations by 6% and 2.4%, respectively over NCR Delhi. On the other hand, the increased atmospheric

stability due to ARF hinders the pollutants outflow and enhances the $PM_{2.5}$ (17.5%) and O_3 (2.5%) concentrations. The synergistic APE and ARF contributed very little (~1%) to the surface O_3 and $PM_{2.5}$ concentration. This study implies that reducing $PM_{2.5}$ concentrations may lead to O_3 escalation due to weakened aerosol radiation interactions. Considering the remarkable impact of APE and ARF on O_3 and $PM_{2.5,}$ these effects need to be considered in designing policies for co-controlling O_3 and $PM_{2.5}$. Reducing VOC emissions (by 50%) results in a decrease in the oxidant levels (38–48% decrease in O_3 and OH) and secondary aerosols (26%) and leads to a 16% $PM_{2.5}$ reduction, highlighting the effectiveness of VOC control in achieving O_3 and $PM_{2.5}$ reductions in Delhi.

This study provides first-hand information on evaluating the APE and ARF effects on O_3 and $PM_{2.5}$ using a meteorology–chemistry modeling framework in Delhi. The elucidation of the role of APE and ARF is particularly significant to understand the complex $PM_{2.5}$–O_3 nexus over polluted regions and the co-benefits attributed to the reduction in both pollutants. However, other factors such as heterogeneous reactions associated with aerosol and aerosol-cloud interactions also need to be considered for further insights into the impact of aerosol radiative effects on O_3 and $PM_{2.5}$ concentration.

Acknowledgments

We sincerely thank NASA Atmospheric Composition Modeling and Analysis Program (ACMAP, award number 80NSSC19K0950) and Multi-Angle Imager for Aerosols (MAIA, award number: H389700) satellite mission for funding this research. The authors acknowledge the High-Performance Computing at the University of Iowa for model simulations.

Open Research

The authors acknowledge the Central Pollution Control Board (CPCB) of India (https://app.cpcbccr.com/ccr/#/caaqm-dashboard-all/caaqm-landing) for $PM_{2.5,}$ O_3, T2, and RH data. WRF-Chem is an open-access model which can be acquired at https://www2.acom.ucar.edu/wrf-chem. The authors thank NASA for making MERRA-2 reanalysis (https://gmao.gsfc.nasa.gov/reanalysis/MERRA-2/) and GLDAS (https://disc.gsfc.nasa.gov/datasets?keywords=GLDAS) data publicly accessible. The EDGAR-

HTAP v2 anthropogenic emissions were obtained from https://edgar.jrc.ec.europa.eu/dataset_htap_v2.

References

Bawase, M., Sathe, Y., Khandaskar, H., & Sukrut, T. (2021). Chemical composition and source attribution of $PM_{2.5}$ and PM_{10} in Delhi-National Capital Region (NCR) of India: results from an extensive seasonal campaign. *J Atmos Chem, 78*, 35–58. https://doi.org/10.1007/s10874-020-09412-7

Benas, N., Mourtzanou, E., Kouvarakis, G., Bais, A., Mihalopoulos, N., & Vardavas, I. (2013). Surface ozone photolysis rate trends in the Eastern Mediterranean: Modeling the effects of aerosols and total column ozone based on Terra MODIS data. *Atmospheric Environment, 74*, 1-9. doi:https://doi.org/10.1016/j.atmosenv.2013.03.019

Bharali, C., Nair, V. S., Chutia, L., & Babu, S. (2019). Modeling of the Effects of Wintertime Aerosols on Boundary Layer Properties Over the Indo Gangetic Plain. *Journal of Geophysical Research: Atmospheres, 124*. doi:10.1029/2018JD029758

Bran, S. H., & Srivastava, R. (2017). Investigation of PM(2.5) mass concentration over India using a regional climate model. *Environ Pollut, 224*, 484-493. doi:10.1016/j.envpol.2017.02.030

Chen, Y., Wild, O., Ryan, E., Sahu, S. K., Lowe, D., Archer-Nicholls, S., . . . Beig, G. (2020). Mitigation of PM2.5 and ozone pollution in Delhi: a sensitivity study during the pre-monsoon period. *Atmos. Chem. Phys., 20*(1), 499-514. doi:10.5194/acp-20-499-2020

Chou, M.-D., & Suarez, M. J. (1994). An efficient thermal infrared radiation parameterization for use in general circulation models. *NASA Technical Memorandum 104606, 3,* 85. https://archive.org/details/nasa_techdoc_19950009331

Chutia, L., Ojha, N., Girach, I. A., Sahu, L. K., Alvarado, L. M. A., Burrows, J. P., . . . Bhuyan, P. K. (2019). Distribution of volatile organic compounds over Indian subcontinent during winter: WRF-chem simulation versus observations. *Environ Pollut, 252*(Pt A), 256-269. doi:10.1016/j.envpol.2019.05.097

Conibear, L., Butt, E. W., Knote, C., Arnold, S. R., & Spracklen, D. V. (2018). Residential energy use emissions dominate health impacts from exposure to ambient particulate matter in India. *Nature Communications, 9*(1), 617. doi:10.1038/s41467-018-02986-7

Dickerson, R. R., Kondragunta, S., Stenchikov, G., Civerolo, K. L., Doddridge, B. G., & Holben, B. N. (1997). The impact of aerosols on solar ultraviolet radiation and photochemical smog. *Science, 278*(5339), 827-830. doi:10.1126/science.278.5339.827

Flynn, J., Lefer, B., Rappenglück, B., Leuchner, M., Perna, R., Dibb, J., . . . Crawford, J. (2010). Impact of clouds and aerosols on ozone production in Southeast Texas. *Atmospheric Environment, 44*(33), 4126-4133. doi:https://doi.org/10.1016/j.atmosenv.2009.09.005

Ge, C., Wang, J., & Reid, J. (2013). Mesoscale modeling of smoke transport over the Southeast Asian Maritime Continent: Coupling of smoke direct radiative feedbacks below and above the low-level clouds. *Atmospheric Chemistry & Physics Discussions, 13*, 15443-15492. doi:10.5194/acpd-13-15443-2013

Ge, C., Wang, J., Reid, J. S., Posselt, D. J., Xian, P., & Hyer, E. J. (2017). Mesoscale modeling of smoke transport from equatorial Southeast Asian Maritime Continent to the Philippines: First comparison of ensemble analysis with in situ observations. *Journal of Geophysical Research, 122*, 5380-5398.

Ghude, S. D., Chate, D. M., Jena, C., Beig, G., Kumar, R., Barth, M. C., . . . Pithani, P. (2016). Premature mortality in India due to PM2.5 and ozone exposure. *Geophysical Research Letters, 43*(9), 4650-4658. doi:https://doi.org/10.1002/2016GL068949

Hakim, Z. Q., Archer-Nicholls, S., Beig, G., Folberth, G. A., Sudo, K., Abraham, N. L., . . . Archibald, A. T. (2019). Evaluation of tropospheric ozone and ozone precursors in simulations from the HTAPII and CCMI model intercomparisons – a focus on the Indian subcontinent. *Atmos. Chem. Phys., 19*(9), 6437-6458. doi:10.5194/acp-19-6437-2019

Janssens-Maenhout, G., Crippa, M., Guizzardi, D., Dentener, F., Muntean, M., Pouliot, G., . . . Li, M. (2015). HTAP_v2.2: a mosaic of regional and global emission grid maps for 2008 and 2010 to study hemispheric transport of air pollution. *Atmos. Chem. Phys., 15*(19), 11411-11432. doi:10.5194/acp-15-11411-2015

Jat, R., Gurjar, B. R., & Lowe, D. (2021). Regional pollution loading in winter months over India using high resolution WRF-Chem simulation. *Atmospheric Research, 249*, 105326. doi:https://doi.org/10.1016/j.atmosres.2020.105326

Krishna, R. K., Ghude, S. D., Kumar, R., Beig, G., Kulkarni, R., Nivdange, S., & Chate, D. (2019). Surface PM2.5 Estimate Using Satellite-Derived Aerosol Optical Depth over India. *Aerosol and Air Quality Research, 19*(1), 25-37. doi:10.4209/aaqr.2017.12.0568

Kulkarni, S. H., Ghude, S. D., Jena, C., Karumuri, R. K., Sinha, B., Sinha, V., . . . Khare, M. (2020). How Much Does Large-Scale Crop Residue Burning Affect the Air Quality in Delhi? *Environ Sci Technol, 54*(8), 4790-4799. doi:10.1021/acs.est.0c00329

Kumar, R., Ghude, S. D., Biswas, M., Jena, C., Alessandrini, S., Debnath, S., . . . Rajeevan, M. (2020). Enhancing Accuracy of Air Quality and Temperature Forecasts During Paddy Crop Residue Burning Season in Delhi Via Chemical Data Assimilation. *Journal of Geophysical Research: Atmospheres, 125*(17), e2020JD033019. doi:https://doi.org/10.1029/2020JD033019

Li, G., Bei, N., Tie, X., & Molina, L. T. (2011). Aerosol effects on the photochemistry in Mexico City during MCMA-2006/MILAGRO campaign. *Atmos. Chem. Phys., 11*(11), 5169-5182. doi:10.5194/acp-11-5169-2011

Li, G., Zhang, R., Fan, J., & Tie, X. (2005). Impacts of black carbon aerosol on photolysis and ozone. *Journal of Geophysical Research: Atmospheres, 110*(D23).

Li, N., He, Q., Greenberg, J., Guenther, A., Li, J., Cao, J., . . . Zhang, Q. (2018). Impacts of biogenic and anthropogenic emissions on summertime ozone formation in the Guanzhong Basin, China. *Atmos. Chem. Phys., 18*(10), 7489-7507. doi:10.5194/acp-18-7489-2018

Li, Z., Guo, J., Ding, A., Liao, H., Liu, J., Sun, Y., . . . Zhu, B. (2017). Aerosol and boundary-layer interactions and impact on air quality. *National Science Review, 4*(6), 810-833. doi:10.1093/nsr/nwx117

Liao, H., Yung, Y., & Seinfeld, J. (1999). Effect of Aerosols on Tropospheric Photolysis Rates in Clear and Cloudy Atmospheres. *Journal of Geophysical Research, 1042*, 23697-23708. doi:10.1029/1999JD900409

Liu, Q., Jia, X., Quan, J., Li, J., Li, X., Wu, Y., . . . Liu, Y. (2018). New positive feedback mechanism between boundary layer meteorology and secondary aerosol formation during severe haze events. *Scientific Reports, 8*(1), 6095. doi:10.1038/s41598-018-24366-3

Mogno, C., Palmer, P. I., Knote, C., Yao, F., & Wallington, T. J. (2021). Seasonal distribution and drivers of surface fine particulate matter and organic aerosol over the Indo-Gangetic Plain. *Atmos. Chem. Phys., 21*(14), 10881-10909. doi:10.5194/acp-21-10881-2021

Mukherjee, T., Vinoj, V., Midya, S. K., Puppala, S. P., & Adhikary, B. (2020). Numerical simulations of different sectoral contributions to post monsoon pollution over Delhi. *Heliyon, 6*(3), e03548. doi:https://doi.org/10.1016/j.heliyon.2020.e03548

Nelson, B. S., Stewart, G. J., Drysdale, W. S., Newland, M. J., Vaughan, A. R., Dunmore, R. E., . . . Lee, J. D. (2021). In situ ozone production is highly sensitive to volatile organic compounds in Delhi, India. *Atmos. Chem. Phys., 21*(17), 13609-13630. doi:10.5194/acp-21-13609-2021

Ojha, N., Sharma, A., Kumar, M., Girach, I., Ansari, T. U., Sharma, S. K., . . . Gunthe, S. S. (2020). On the widespread enhancement in fine particulate matter across the Indo-Gangetic Plain towards winter. *Sci Rep, 10*(1), 5862. doi:10.1038/s41598-020-62710-8

Qu, Y., An, J., & Li, J. (2013). Synergistic impacts of anthropogenic and biogenic emissions on summer surface O3 in East Asia. *Journal of Environmental Sciences, 25*(3), 520-530. doi:https://doi.org/10.1016/S1001-0742(12)60069-2

Real, E., & Sartelet, K. (2011). Modeling of photolysis rates over Europe: impact on chemical gaseous species and aerosols. *Atmos. Chem. Phys., 11*(4), 1711-1727. doi:10.5194/acp-11-1711-2011

Reid, J. S., Hyer, E. J., Prins, E. M., Westphal, D. L., Zhang, J., Wang, J., . . . Hoffman, J. P. (2009). Global Monitoring and Forecasting of Biomass-Burning Smoke: Description of and Lessons From the Fire Locating and Modeling of Burning Emissions (FLAMBE) Program. *IEEE Journal of Selected Topics in Applied Earth Observations and Remote Sensing, 2*(3), 144-162. doi:10.1109/JSTARS.2009.2027443

Sahu, S. K., & Kota, S. H. (2017). Significance of PM2.5 Air Quality at the Indian Capital. *Aerosol and Air Quality Research, 17*(2), 588-597. doi:10.4209/aaqr.2016.06.0262

Schell, B., Ackermann, I. J., Hass, H., Binkowski, F. S., & Ebel, A. (2001). Modeling the formation of secondary organic aerosol within a comprehensive air quality model system. *Journal of Geophysical Research: Atmospheres, 106*(D22), 28275-28293.

Sha, T., Ma, X., Zhang, H., Janechek, N., Wang, Y., Wang, Y., . . . Wang, J. (2021). Impacts of Soil NOx Emission on O3 Air Quality in Rural California. *Environmental Science & Technology, 55*(10), 7113-7122. doi:10.1021/acs.est.0c06834

Sharma, A., Ojha, N., Pozzer, A., Mar, K. A., Beig, G., Lelieveld, J., & Gunthe, S. S. (2017). WRF-Chem simulated surface ozone over south Asia during the pre-monsoon: effects of emission inventories and chemical mechanisms. *Atmos. Chem. Phys., 17*(23), 14393-14413. doi:10.5194/acp-17-14393-2017

Sinha, B., Singh Sangwan, K., Maurya, Y., Kumar, V., Sarkar, C., Chandra, B. P., & Sinha, V. (2015). Assessment of crop yield losses in Punjab and Haryana using 2 years of continuous in situ ozone measurements. *Atmos. Chem. Phys., 15*(16), 9555-9576. doi:10.5194/acp-15-9555-2015

Stein, U., & Alpert, P. (1993). Factor Separation in Numerical Simulations. *Journal of Atmospheric Sciences, 50*(14), 2107-2115. doi:10.1175/1520-0469(1993)050<2107:Fsins>2.0.Co;2

Stockwell, W. R., Middleton, P., Chang, J. S., & Tang, X. (1990). The second generation regional acid deposition model chemical mechanism for regional air quality modeling. *Journal of Geophysical Research: Atmospheres, 95*(D10), 16343-16367.

Tie, X., Madronich, S., Walters, S., Zhang, R., Rasch, P., & Collins, W. (2003). Effect of clouds on photolysis and oxidants in the troposphere. *Journal of Geophysical Research: Atmospheres, 108*(D20). doi:https://doi.org/10.1029/2003JD003659

Upadhyay, A., Dey, S., Chowdhury, S., & Goyal, P. (2018). Expected health benefits from mitigation of emissions from major anthropogenic PM2.5 sources in India: Statistics at state level. *Environmental Pollution, 242*, 1817-1826. doi:https://doi.org/10.1016/j.envpol.2018.07.085

Wang, J., Ge, C., Yang, Z., Hyer, E. J., Reid, J. S., Chew, B.-N., . . . Zhang, M. (2013). Mesoscale modeling of smoke transport over the Southeast Asian Maritime Continent: Interplay of sea breeze, trade wind, typhoon, and topography. *Atmospheric Research, 122*, 486-503. doi:10.1016/j.atmosres.2012.05.009

Wang, Y., Yu, M., Wang, Y., Tang, G., Song, T., Zhou, P., . . . Petäjä, T. (2020). Rapid formation of intense haze episodes via aerosol–boundary layer feedback in Beijing. *Atmos. Chem. Phys., 20*(1), 45-53. doi:10.5194/acp-20-45-2020

Wu, J., Bei, N., Hu, B., Liu, S., Wang, Y., Shen, Z., . . . Li, G. (2020). Aerosol-photolysis interaction reduces particulate matter during wintertime haze events. *Proc Natl Acad Sci U S A, 117*(18), 9755-9761. doi:10.1073/pnas.1916775117

Xing, J., Wang, J., Mathur, R., Wang, S., Sarwar, G., Pleim, J., . . . Hao, J. (2017). Impacts of aerosol direct effects on tropospheric ozone through changes in atmospheric dynamics and photolysis rates. *Atmos. Chem. Phys., 17*(16), 9869-9883. doi:10.5194/acp-17-9869-2017

Yang, H., Chen, L., Liao, H., Zhu, J., Wang, W., & Li, X. (2022). Impacts of aerosol–photolysis interaction and aerosol–radiation feedback on surface-layer ozone in North China during multi-pollutant air pollution episodes. *Atmos. Chem. Phys., 22*(6), 4101-4116. doi:10.5194/acp-22-4101-2022

Yang, Y., Chen, M., Zhao, X., Chen, D., Fan, S., Guo, J., & Ali, S. (2020). Impacts of aerosol–radiation interaction on meteorological forecasts over northern China by offline coupling of the WRF-Chem-simulated aerosol optical depth into WRF: a case study during a heavy pollution event. *Atmos. Chem. Phys., 20*(21), 12527-12547. doi:10.5194/acp-20-12527-2020

Zhang, H., Wang, J., García, L. C., Zhou, M., Ge, C., Plessel, T., . . . Spero, T. L. (2022). Improving Surface PM2.5 Forecasts in the United States Using an Ensemble of Chemical Transport Model Outputs: 2. Bias Correction With Satellite Data for Rural Areas. *Journal of Geophysical Research: Atmospheres, 127*(1), e2021JD035563. doi:https://doi.org/10.1029/2021JD035563

Zhao, D., Xin, J., Gong, C., Quan, J., Liu, G., Zhao, W., . . . Song, T. (2019). The formation mechanism of air pollution episodes in Beijing city: Insights into the measured feedback between aerosol radiative forcing and the atmospheric boundary layer stability. *Science of The Total Environment, 692*, 371-381. doi:https://doi.org/10.1016/j.scitotenv.2019.07.255